Relativistic effects in proton-antiproton annihilation into two mesons

Relativistic effects in proton-antiproton annihilation into two mesons

M. Maruyama,* T. Gutsche, Amand Faessler, and G. L. Strobel†
Institut für Theoretische Physik, Universität Tübingen, Auf der Morgenstelle 14, 7400 Tübingen, Federal Republic of Germany
(Received 18 September 1989)

The effects of the small components of Dirac spinors, used to describe quark and antiquark wave functions in clusters, and the Lorentz contraction of cluster wave functions associated with the Lorentz transformation to the overall center of momentum frame are considered in the proton-antiproton annihilation into two final state mesons. A quark-antiquark pair annihilation and creation model in the planar picture that reproduces the principly observed final states in the nonrelativistic case is used. The effects are studied by taking the nonrelativistic model as a base of comparison. The introduction of small components in the quark wave functions has little influence on predictions of relative ratios of annihilation amplitudes into final state mesons in the same relative angular momentum state of the initial proton and antiproton. In contrast, the small components give a large contribution to the absolute value of the annihilation amplitude in dependence on the initial relative angular momentum. The effects of including the Lorentz contraction of the cluster wave functions appear in the annihilation amplitudes of two meson final states. By using Lorentz transformed Gaussian wave functions for the clusters, subsequent effects on the annihilation amplitudes into two mesons, such as $\pi\pi$, $\rho\pi$, and $\rho\rho$, are studied. For a nucleon radius of $\langle r^2\rangle_N^{1/2}=0.62$ fm and a global meson radius of $\langle r^2\rangle_M^{1/2}=0.50$ fm, the production of two final state pions is enhanced upon including the Lorentz contraction effects.

I. INTRODUCTION

The nucleon-antinucleon interaction can be described theoretically by a meson exchange interaction dominant in the long and intermediate range and by a short range annihilation into mesons. The first attempts to explain the annihilation using a nonrelativistic quark model were made by Rubinstein and Stern,[1] and by Harte, Socolow, and Vandermeulen,[2] which, however, in their simplistic approach failed to reproduce the experimental meson branching ratios. Maruyama and Ueda[3-5] have proposed a new model which can explain the general features of experimental meson branching ratios from proton-antiproton ($P\bar{P}$) annihilation at low energies. This model indicates that the spatial part of the cluster wave functions of the quarks and antiquarks in the proton, antiproton, and the final state mesons plays a crucial role in calculations that are subsequently able to reproduce the experimental data. The importance of the spatial part of the meson wave function in explaining experimental numbers has also been noticed in hadron spectroscopy[6-8] and hadron decay and reaction[9-11] studies.

Antiproton annihilation on hydrogen can be modeled in several ways,[12] specifically by various quark models based on the planar and nonplanar topology of the flavor flux.[3-5,13-22] Quark rearrangement and annihilation models as defined by the different quark diagram topologies have evolved in the literature. Possible annihilation/creation vertices considered are the scalar ($^3P_0$) or the vector vertex ($^3S_1$). Many calculations of meson decays have been carried out by using the scalar[23] and the vector[24] interaction. In principle it is not so obvious whether the same vertex can be applied in both nucleon-antinucleon annihilation and meson decay processes, since the structure of the color flux and the available energy scale are different. The current state of the calculational art for the proton-antiproton annihilation focuses on branching ratios for various final meson states in comparison of theoretical models with experimental data.

Usually a nonrelativistic Hamiltonian approach is used to describe the quark dynamics within the initial and final state clusters.[3-5,12-19] The effects of the small component on the $q\bar{q}$ annihilation/creation vertex have been studied by extracting an effective $q\bar{q}$ annihilation/creation vertex from the one-gluon exchange interaction in some recent works.[20-22] However, other possible relativistic effects as contained in the small component of a quark Dirac spinor and in the Lorentz boost of the quark wave functions are neglected. Velocities of the final state mesons are in the relativistic region, even for low relative momenta of the initial proton-antiproton system. In the $P\bar{P}$ annihilation into two mesons at rest, two pions or two ρ mesons, for example, the final state mesons are moving quite relativistically in the overall center of momentum frame ($v_\pi/c\approx 99\%$ and $v_\rho/c\approx 60\%$).

The study of the relativistic effects becomes very important when considering the relation of a nonrelativistic quark annihilation model to quark models for other hadron reactions or to more fundamental theories, and when consequently discussing the physical meaning of the parameters appearing in the model. The effects would depend on the scale of the available energy, or on the velocities of the hadrons appearing in the reaction. They have to be estimated when extracting the fundamental quanti-

ties from the model determining the physics of the system.

It is the purpose of this paper to propose a relativistic quark annihilation model that agrees with the conventional quark annihilation model in the nonrelativistic limit. The effects of including the small components of a Dirac spinor for the quark wave functions are studied. The quark momentum couples to the spin in the small components of the quark wave function. Therefore, inclusion of the small components changes the spin-flavor structure of the annihilation amplitudes. We estimate the corrections to the spin-flavor matrix elements due to the small components. The effects of Lorentz contraction on the cluster wave functions are treated in an approximate fashion. Lorentz boosts transform the large and small components of a free Dirac particle into each other in a well-known way.[25] Here we assume that quarks in the rest frame of a cluster are described by a Gaussian ansatz wave function for their motion relative to the center of the cluster. We study the effects of Lorentz contraction associated with the Lorentz transformations from the cluster rest frame to the overall center of momentum frame. This follows prior studies[25–30] on Lorentz contraction effects in electromagnetic form factors of proton clusters.

Due to kinematical reasons relativistic effects are most important in the $P\bar{P}$ annihilation into two mesons. Here we consider the planar $A2$ model with the scalar vertex (see Fig. 1) for the annihilation into two mesons, as this model, combined with the $R3$ or the $A3$ diagram (Fig. 2) for the annihilation into three mesons, suitably describes the branching ratios of the major two-body final state channels seen in $P\bar{P}$ annihilation.[17,18,31]

In Sec. II a relativistic quark model including the effects of small components for nucleon-antinucleon annihilation into two mesons is proposed. The transition

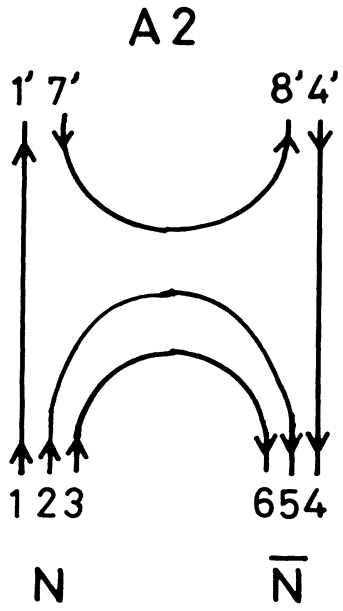

FIG. 1. The $A2$ diagram with two $q\bar{q}$ pair annihilations and one pair creation for proton-antiproton annihilation into two mesons.

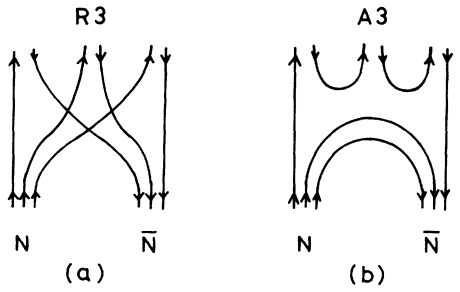

FIG. 2. Proton-antiproton annihilation into three mesons. (a) Nonplanar diagram ($R3$) and (b) planar diagram ($A3$).

matrix elements of the process are presented. Section III is devoted to construct the annihilation amplitudes including the effects of Lorentz contraction on cluster wave functions. In Sec. IV the results of both the relativistic extensions are shown in comparison with the conventional nonrelativistic model. We summarize our results in Sec. V.

II. THE EFFECTS OF THE SMALL COMPONENTS

In the absence of center of momentum corrections (i.e., without projections onto a fixed total nucleon momentum) the quark cluster wave function in the nucleon ground state is simply described by a product state of three valence quarks occupying $1s_{1/2}$ orbits. In defining the individual quark wave function we take a Dirac spinor wave function with a Gaussian form as[32]

$$\psi_q(\mathbf{r})=\frac{1}{\sqrt{R_N^3\pi^{3/2}(1+\frac{3}{2}\beta_N^2)}}\exp\left[-\frac{r^2}{2R_N^2}\right]\times\begin{bmatrix}\chi\\ i\beta_N\dfrac{\boldsymbol{\sigma}\cdot\mathbf{r}}{R_N}\chi\end{bmatrix}, \tag{2.1}$$

where σ is the Pauli spin matrix and χ is a two-component spinor. The wave function is normalized by

$$\int d^3r\,\psi_q^\dagger(\mathbf{r})\psi_q(\mathbf{r})=1\ , \tag{2.2}$$

and the root mean square (rms) radius of the single quark wave function is given by

$$\sqrt{\langle r^2\rangle}=\left[\tfrac{3}{2}R_N^2\left[\frac{1+\frac{5}{2}\beta_N^2}{1+\frac{3}{2}\beta_N^2}\right]\right]^{1/2}. \tag{2.3}$$

There are two adjustable quantities to this wave function, which in the case of the nucleon are the nucleon size R_N and the weight of the small component β_N. Following Wong,[32] the Gaussian expression is an approximation to the $1s_{1/2}$ quark wave function in the bag. Then the value of β_N is taken to be 0.36, which fits the probability of the lower component in the bag model,[32] and is also comparable to the axial to vector coupling ratio for the proton.[33] [The probability of the lower component is given by $\frac{3}{2}\beta_N^2/(1+\frac{3}{2}\beta_N^2)$, which for the given value of $\beta_N=0.36$ results in an axial charge $g_A/g_V=1.30$.] In a slight modification to Ref. 32 the radial parameter R_N is adjust-

ed to the value of 0.62 fm (compared to $R_N=0.57$ fm of Ref. 32) as determined by the static properties of the nucleon in a nonrelativistic model,[6] and therefore reproduces the rms size of the quark component closely when the center of momentum motion of the nucleon cluster wave function is removed. Figure 3 depicts the single quark wave function given in Eq. (2.1) compared to the MIT bag wave function.[34] This wave function agrees with the nonrelativistic wave function used in Refs. 4 and 17 in the limit that β_N goes to zero, that is, when the small component is neglected.

In principle, the single quark wave function of Gaussian form can also be derived from the Dirac equation with a given confining potential of Lorentz scalar and/or vector nature.[35,36] Work along this line, with the choice of somewhat different model parameters, was applied successfully to the description of the nucleon ground state properties including the electromagnetic form factors[35] and of the baryonic mass spectrum.[36]

A single quark (antiquark) has two components $u^{(i)}$ [$v^{(i)}$] ($i=1,2$) in which $i=1,2$ stands for the upper and lower components in Eq. (2.1)

$$\psi_q(\mathbf{r})=\begin{bmatrix} u^{(1)}(\mathbf{r}) \\ u^{(2)}(\mathbf{r}) \end{bmatrix}, \quad \left[\psi_{\bar{q}}(\mathbf{r})=\begin{bmatrix} v^{(1)}(\mathbf{r}) \\ v^{(2)}(\mathbf{r}) \end{bmatrix} \right] . \tag{2.4}$$

Therefore a nucleon cluster is described by a product of three quark wave functions and thus is a $2^3=8$ component wave function $\Phi_N^{(ijk)}=u^{(i)}u^{(j)}u^{(k)}$ $(i,j,k=1,2)$. The resulting wave function is not a center of momentum eigenstate. The Peierls-Yoccoz method[32] is used to treat the center of momentum motion problem associated with single-body wave functions in a cluster. In this work we use plane waves as a base for the center of momentum motions of nucleon and meson clusters. For a nucleon cluster wave function, describing the three quark momenta as $\mathbf{q}_1$, $\mathbf{q}_2$, and $\mathbf{q}_3$, we obtain in momentum space

$$\Phi_N^{(ijk)}(\mathbf{P}_N,\mathbf{q}_1,\mathbf{q}_2,\mathbf{q}_3)=\delta^3(\mathbf{P}_N-\mathbf{q}_1-\mathbf{q}_2-\mathbf{q}_3) \times\phi_N^{(ijk)}(P_N,\mathbf{q}_1,\mathbf{q}_2,\mathbf{q}_3) , \tag{2.5}$$

where $\mathbf{P}_N$ and P_N are the nucleon momentum and its absolute value, respectively. In the Appendix the internal part $\phi_N^{(ijk)}(P_N,\mathbf{q}_1,\mathbf{q}_2,\mathbf{q}_3)$ is given explicitly with the center of momentum motion being removed, following the Peierls-Yoccoz method.[32] For an antiquark in the initial state we take

$$\psi_{\bar{q}}^{\dagger}(\mathbf{r})=\frac{1}{\sqrt{R_N^3\pi^{3/2}(1+\frac{3}{2}\beta_N^2)}} \times\exp\left[-\frac{r^2}{2R_N^2}\right]\left[\tilde{\chi}^{\dagger}i\beta_N\frac{\boldsymbol{\sigma}\cdot\mathbf{r}}{R_N},\tilde{\chi}^{\dagger}\right], \tag{2.6}$$

where $\tilde{\chi}$ is a two-component spinor

$$\tilde{\chi}=\begin{bmatrix} 0 \\ -1 \end{bmatrix} \text{ for spin projection}=\tfrac{1}{2}$$
$$=\begin{bmatrix} 1 \\ 0 \end{bmatrix} \text{ for spin projection}=-\tfrac{1}{2} . \tag{2.7}$$

[The respective transformation to the antiquark state by charge conjugation with chosen phase convention is given by $\psi_{\bar{q}}=C\bar{\psi}_q^T=(-i)\gamma^2\gamma^4\bar{\psi}_q^T$.] The initial state wave function of an antiquark is described by a row vector instead of a column vector for a quark. The resulting wave functions for an antinucleon and a meson are

$$\Phi_{\bar{N}}^{(ijk)\dagger}(\mathbf{P}_{\bar{N}},\mathbf{q}_4,\mathbf{q}_5,\mathbf{q}_6)=\delta^3(\mathbf{P}_{\bar{N}}-\mathbf{q}_4-\mathbf{q}_5-\mathbf{q}_6) \times\phi_{\bar{N}}^{(ijk)^{\dagger}}(P_{\bar{N}},\mathbf{q}_4,\mathbf{q}_5,\mathbf{q}_6) \tag{2.8}$$

and

$$\Phi_{\alpha}^{(ij)}(\mathbf{p}_{\alpha},\mathbf{q}_1,\mathbf{q}_7)=\delta^3(\mathbf{p}_{\alpha}-\mathbf{q}_1-\mathbf{q}_7)\phi_{\alpha}^{(ij)}(p_{\alpha},\mathbf{q}_1,\mathbf{q}_7) , \tag{2.9}$$

where $\mathbf{P}_{\bar{N}}$ and $\mathbf{p}_{\alpha}$ are the momenta of the antinucleon and meson, respectively. $\mathbf{q}_4$, $\mathbf{q}_5$, and $\mathbf{q}_6$ [Eq. (2.8)] are the antiquark momenta in the antinucleon cluster, and $\mathbf{q}_1$ and $\mathbf{q}_7$ [Eq. (2.9)] are the quark and antiquark momenta in the meson cluster. The explicit expressions for $\phi_{\bar{N}}^{(ijk)\dagger}$ and $\phi_{\alpha}^{(ij)}$ are shown in the Appendix. Here we consider the s-wave

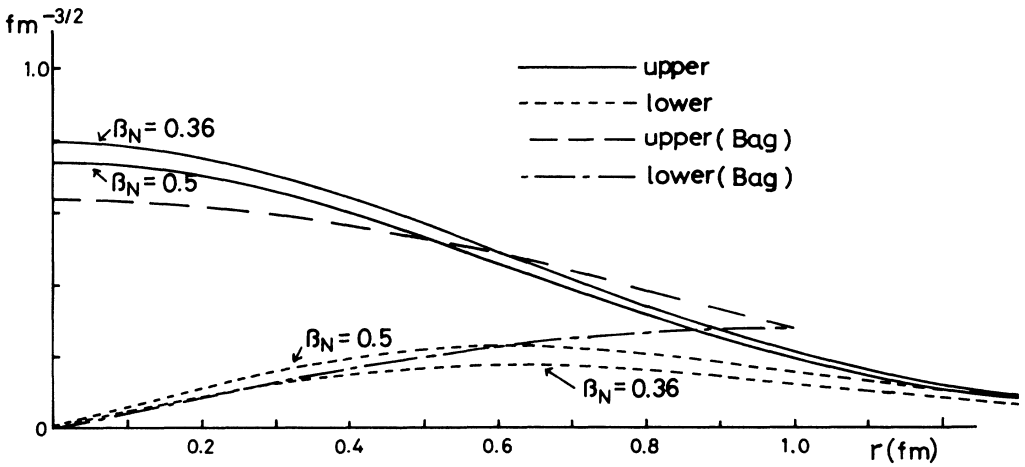

FIG. 3. The single quark wave function defined in Eq. (2.1). The solid curve is the upper component and the dotted curve is the lower component ($R_N=0.62$ fm, $\beta_N=0.36$ and 0.5). The dashed and dotted-dashed curves are the upper and lower components of the MIT bag wave function for a bag radius of 1 fm.

mesons π, η, ρ, and ω as the final state mesons. The meson size and the weight of the small components in the meson cluster wave function are R_m and β_m, respectively. The parameter R_m is taken as 0.57 fm, which sets the meson size to 0.5 fm.[17]

We use the $A2$ model depicted in Fig. 1 to describe $P\bar{P}$ annihilation into two mesons. Quark-antiquark ($q\bar{q}$) pairs are assumed to create out of and annihilate into the vacuum ($^3P_0$ vertex). In the relativistic model the vertex is analogous to a scalar interaction for the Dirac spinors of the annihilating quark and antiquark. For example, the vertex for the pair annihilation of the quark $\{2\}$ and the antiquark $\{5\}$ in Fig. 1 is written as

$$\begin{aligned}\bar{\psi}_{\bar{q}}(5)\psi_q(2)&=\psi_{\bar{q}}(5)^\dagger\gamma_4\psi_q(2)\\&=\sum_{i,j=1}^{2} v^{(i)}(5)^\dagger(-1)^{1+i}\delta_{i,j}u^{(j)}(2)\\&=v^{(1)}(5)^\dagger u^{(1)}(2)-v^{(2)}(5)^\dagger u^{(2)}(2)\ .\end{aligned}\tag{2.10}$$

For single quark wave functions which have the following form in momentum space as

$$\begin{aligned}\psi_q(\mathbf{q}_2)&\propto\begin{bmatrix}\chi^{(2)}\\ \beta R\,\boldsymbol{\sigma}^{(2)}\cdot\mathbf{q}_2\chi^{(2)}\end{bmatrix},\\ \psi_{\bar{q}}(\mathbf{q}_5)&\propto\begin{bmatrix}\beta R\,\boldsymbol{\sigma}^{(5)}\cdot\mathbf{q}_5\tilde{\chi}^{(5)}\\ \tilde{\chi}^{(5)}\end{bmatrix},\end{aligned}\tag{2.11}$$

this vertex coincides with the $^3P_0$ vertex in the nonrelativistic quark model,

$$\bar{\psi}_{\bar{q}}(\mathbf{q}_5)\psi_q(\mathbf{q}_2)\propto\beta R\,\tilde{\chi}^{(5)\dagger}\boldsymbol{\sigma}^{(2)}\cdot(\mathbf{q}_5-\mathbf{q}_2)\chi^{(2)}\ .\tag{2.12}$$

Including the effects of the small components, the transition amplitude T of nucleon-antinucleon annihilation into two mesons is simply given by the overlap of the final and initial state wave functions with the appropriate quark-antiquark (quark) pairs contracted by a scalar interaction according to Fig. 1. The amplitude T is defined as

$$\begin{aligned}T=&\sum_{i_1\cdots i_6,i_1',i_4',i_7',i_8'}\int d^3q_1'd^3q_4'd^3q_7'd^3q_8'd^3q_1\cdots d^3q_6\,\Phi_{\bar{N}}^{(i_4i_5i_6)\dagger}\Phi_\beta^{(i_8'i_4')\dagger}\Phi_\alpha^{(i_1'i_7')\dagger}\Phi_N^{(i_1i_2i_3)}\\&\times\lambda_{A2}(-1)^{1+i_1}\delta_{i_1,i_1'}\delta^3(\mathbf{q}_1'-\mathbf{q}_1)(-1)^{1+i_4}\delta_{i_4,i_4'}\delta^3(\mathbf{q}_4'-\mathbf{q}_4)\\&\times(-1)^{1+i_2}\delta_{i_2,i_5}\delta^3(\mathbf{q}_2+\mathbf{q}_5)(-1)^{1+i_3}\delta_{i_3,i_6}\delta^3(\mathbf{q}_3+\mathbf{q}_6)(-1)^{1+i_7'}\delta_{i_7',i_8'}\delta^3(\mathbf{q}_7'+\mathbf{q}_8')\\=&N_{N\bar{N}\alpha\beta}\delta^3(\mathbf{P}_N+\mathbf{P}_{\bar{N}}-\mathbf{p}_\alpha-\mathbf{p}_\beta)\exp\left[-\frac{3R_N^2R_m^2}{2(3R_N^2+4R_m^2)}(\mathbf{p}_\alpha-\tfrac{2}{3}\mathbf{P}_N)^2\right]\\&\times\lambda_{A2}(2\beta_NR_N)^2(2\beta_mR_m)\left[\frac{\pi^2}{AB}\right]^{3/2}\frac{(3R_N^2+2R_m^2)(R_N^2+2R_m^2)}{B(3R_N^2+4R_m^2)(R_N^2+R_m^2)}M_{\alpha\beta}(\beta_N\beta_m)\ ,\end{aligned}\tag{2.13}$$

where

$$A=\tfrac{1}{2}(R_N^2+R_m^2),\quad B=\frac{2R_N^2(3R_N^2+4R_m^2)}{(R_N^2+R_m^2)}\ .\tag{2.14}$$

Here λ_{A2} is an adjustable parameter in the model, expressing the strength of the $A2$ diagram. The delta functions in Eq. (2.13) describe the momentum conservation of the spectator and annihilated/created particles during the process. The normalization factor $N_{N\bar{N}\alpha\beta}$ is given in the Appendix. We restrict ourselves to the terms linear in the momenta $\mathbf{P}_N$ or $\mathbf{p}_\alpha$, which correspond to the two transitions, $L_i=0$, $l_f=1$ and $L_i=1$, $l_f=0$, where L_i and l_f are the relative angular momenta of the initial proton-antiproton and the final two-meson state, respectively. With the limitation to the dominant on-shell terms[17] the spin-flavor matrix element $M_{\alpha\beta}(\beta_N\beta_m)$ can then be written as

$$\begin{aligned}M_{\alpha\beta}(\beta_N\beta_m)=&\boldsymbol{\sigma}^{(2)}\cdot\boldsymbol{\sigma}^{(3)}\boldsymbol{\sigma}^{(7)}\cdot\mathbf{p}_\alpha[1+(\beta_N\beta_m)W_{(1)}^m]+(\boldsymbol{\sigma}^{(2)}\cdot\boldsymbol{\sigma}^{(7)}\boldsymbol{\sigma}^{(3)}\cdot\mathbf{p}_\alpha+\boldsymbol{\sigma}^{(3)}\cdot\boldsymbol{\sigma}^{(7)}\boldsymbol{\sigma}^{(2)}\cdot\mathbf{p}_\alpha)C_{(2)}^m[1+(\beta_N\beta_m)W_{(2)}^m]\\&+\boldsymbol{\sigma}^{(2)}\cdot\boldsymbol{\sigma}^{(3)}\boldsymbol{\sigma}^{(7)}\cdot\mathbf{P}_NC_{(1)}^N[1+(\beta_N\beta_m)W_{(1)}^N]\\&+(\boldsymbol{\sigma}^{(2)}\cdot\boldsymbol{\sigma}^{(7)}\boldsymbol{\sigma}^{(3)}\cdot\mathbf{P}_N+\boldsymbol{\sigma}^{(3)}\cdot\boldsymbol{\sigma}^{(7)}\boldsymbol{\sigma}^{(2)}\cdot\mathbf{P}_N)C_{(2)}^N[1+(\beta_N\beta_m)W_{(2)}^N]+O((\beta_N\beta_m)^2)\ ,\end{aligned}\tag{2.15}$$

where

$$W^m_{(1)}=-\frac{4R_NR_m(3R_N^4+9R_N^2R_m^2+2R_m^4)}{(3R_N^2+4R_m^2)(3R_N^2+2R_m^2)(R_N^2+2R_m^2)},$$

$$W^m_{(2)}=-\frac{14R_NR_m}{(3R_N^2+4R_m^2)},$$

$$C^m_{(2)}=\frac{R_N^2R_m^2}{(3R_N^2+2R_m^2)(R_N^2+2R_m^2)},$$

$$W^N_{(1)}=-\frac{4R_NR_m(2R_N^2+5R_m^2)}{(3R_N^2+4R_m^2)(R_N^2+2R_m^2)},\tag{2.16}$$

$$W^N_{(2)}=-\frac{4R_NR_m(2R_N^2+5R_m^2)}{(3R_N^2+4R_m^2)(R_N^2+2R_m^2)},$$

$$C^N_{(1)}=C^N_{(2)}=-\frac{R_N^2}{(3R_N^2+2R_m^2)}.$$

In the expression Eq. (2.15) the terms containing $(\beta_N\beta_m)^n$ represent the effects of the small components. Ignoring these terms, we obtain the nonrelativistic limit of the spin-flavor matrix elements which then agree with those of Ref. 17. Here the terms up to the order $(\beta_N\beta_m)^n$ $(n=1)$ are shown explicitly. The complete expression contains second-order terms $(\beta_N\beta_m)^2$ in addition, which are included in our numerical calculation. We find that the contribution from the second-order terms is less than 10% of the total value for an appropriate and reasonable choice of β_N and β_m. Since the combined value of $(\beta_N\beta_m)W^{m,N}_{(i)}$ is negative, the inclusion of small components decreases the magnitude of the spin-flavor part of the annihilation amplitude.

In the derivation of the previous relativistic extension of the $A2$ model we have also used the scalar interaction

$$\bar{\psi}_q(1')\psi_q(1)=u^{(1)\dagger}(1')u^{(1)}(1)-u^{(2)\dagger}(1')u^{(2)}(1)\tag{2.17}$$

for the continuous quark $\{1\}$ and antiquark $\{4\}$ lines of the $A2$ diagram as well as for the $q\bar{q}$ pair annihilation and creation [Eq. (2.10)]. In principle another treatment of the continuous quark (antiquark) lines has to be considered. If the continuous particles are assumed to be noninteracting during the annihilation process, i.e., they are "true" spectators, the operators $\bar{\psi}_q\psi_q$ for the quark $\{1\}$ and the antiquark $\{4\}$ would be replaced by

$$\bar{\psi}_q(1')\gamma^4\psi_q(1)=\psi^\dagger_q(1')\psi_q(1)$$
$$=u^{(1)\dagger)}(1')u^{(1)}(1)+u^{(2)\dagger}(1')u^{(2)}(1).\tag{2.18}$$

In this case the overlap of the initial and final state quark wave functions for the spectator particles is unity. Using the same scalar operators of Eq. (2.10) for $q\bar{q}$ annihilation and creation, the final result for the transition amplitude is also given by Eqs. (2.13)–(2.16) after replacing $(\beta_N\beta_m)$ by $-(\beta_m\beta_m)$ due to the additional γ^4 structure. Without loss of generality β_N and β_m in the single-particle wave function can be chosen as positive numbers. Negative values for β_N and β_m would just correspond to the Hermitian conjugate of the cluster wave functions, thereby leaving the final result for observables unchanged. Thus effectively in the formalism positive values for $(\beta_N\beta_m)$ correspond to a scalar interaction of the continuous lines [Eq. (2.17)], whereas negative values for $(\beta_N\beta_m)$ describe the probability distribution of the "true" spectators [Eq. (2.18)]. In the latter case the overall positive result for $(\beta_N\beta_m)W^{m,N}_{(i)}$ leads to an increase in the magnitude of the spin-flavor part, contrary to the previous case with a positive value for $(\beta_N\beta_m)$.

Both relativistic interaction forms in the treatment of the continuous quark (antiquark) lines have a common nonrelativistic limit when absorbing overall constants in the strength of the annihilation, parametrized by λ_{A2}. Thus *a priori* both interaction forms have rightfully to be considered, since both result in the nonrelativistic planar $A2$ model. Numerical results for the transition amplitude applying both alternative definitions will be discussed later on.

III. THE EFFECTS OF THE LORENTZ CONTRACTION

We take the point of view that the cluster wave functions are described by a Gaussian in the rest frame of the cluster. In a frame where the cluster is moving the wave function for the cluster will be Lorentz contracted in the direction parallel to the cluster momentum.

The nucleon-antinucleon annihilation amplitude into two mesons (see Fig. 1) that we consider can be written as

$$T=\int d^3q_1'd^3q_4'd^3q_7'd^3q_8'd^3q_1\cdots d^3q_6\Psi_f^\dagger O_{A2}\Psi_i.\tag{3.1}$$

The $N\bar{N}$ initial state wave function is defined as

$$\Psi_i=\delta^3(\mathbf{P}_N-\mathbf{q}_1-\mathbf{q}_2-\mathbf{q}_3)\phi_N(P_N,\mathbf{q}_1,\mathbf{q}_2,\mathbf{q}_3)$$
$$\times\delta^3(\mathbf{P}_{\bar{N}}-\mathbf{q}_4-\mathbf{q}_5-\mathbf{q}_6)\phi_{\bar{N}}(P_{\bar{N}},\mathbf{q}_4,\mathbf{q}_5,\mathbf{q}_6),\tag{3.2}$$

and the wave function for the final two-meson state is given by

$$\Psi_f=\delta^3(\mathbf{p}_\alpha-\mathbf{q}_1'-\mathbf{q}_7')\phi_\alpha(p_\alpha,\mathbf{q}_1',\mathbf{q}_7')$$
$$\times\delta^3(\mathbf{p}_\beta-\mathbf{q}_4'-\mathbf{q}_8')\phi_\beta(p_\beta,\mathbf{q}_4',\mathbf{q}_8').\tag{3.3}$$

In this section we use nonrelativistic two-component spinors for the single quark wave functions as a starting point instead of using Dirac four component spinors as applied in Sec. II. ϕ_N, $\phi_{\bar{N}}$, ϕ_α, and ϕ_β stand for the cluster wave functions and are given by the large cluster components $\phi_N^{(111)}$, $\phi_{\bar{N}}^{(222)\dagger}$, $\phi_\alpha^{(21)}$, and $\phi_\beta^{(21)}$, defined in Sec. II, respectively (see also the Appendix), with the Lorentz contraction effects at this stage not being considered yet. The extension to cluster wave functions including small components are straightforward. Each of the cluster wave functions in the initial and in the final state undergoes a Lorentz contraction along their individual directions of momenta. O_{A2} is an operator which represents the $A2$ annihilation diagram (Fig. 1), describing two initial state quark-antiquark $(q\bar{q})$ annihilations into and a single final state $q\bar{q}$ pair creation out of the vacuum:

$$O_{A2}=\tilde{\lambda}_{A2}\delta^3(\mathbf{q}_1'-\mathbf{q}_1)\delta^3(\mathbf{q}_4'-\mathbf{q}_4)\delta^3(\mathbf{q}_2+\mathbf{q}_5)\sigma^{(2)}\cdot(\mathbf{q}_2-\mathbf{q}_5)$$
$$\times\delta^3(\mathbf{q}_3+\mathbf{q}_6)\sigma^{(3)}\cdot(\mathbf{q}_3-\mathbf{q}_6)\delta^3(\mathbf{q}_7'+\mathbf{q}_8')\sigma^{(7)}\cdot(\mathbf{q}_7'-\mathbf{q}_8').\tag{3.4}$$

The nonrelativistic amplitude in Eq. (3.1) coincides with the relativistic amplitude, including the small component, in Eq. (2.13) in the limit that the terms depending on $(\beta_N\beta_m)$ are ignored in $M_{\alpha\beta}(\beta_N\beta_m)$. The strength parameter $\tilde{\lambda}_{A2}$ can then be related to λ_{A2} in Eq. (2.13) by

$$\tilde{\lambda}_{A2}=-(\beta_N R_N)^2(\beta_m R_m)\lambda_{A2} . \tag{3.5}$$

We work in the overall center of momentum frame where the nucleon and antinucleon have opposite momenta $\mathbf{P}_{\bar{N}}=-\mathbf{P}_N$. Also, the final meson clusters have opposite momenta $\mathbf{p}_\beta=-\mathbf{p}_\alpha$, where $\mathbf{p}_\alpha$ is not necessarily parallel to $\mathbf{P}_N$.

Each of the clusters is moving in the center of momentum frame. We use "tilded" coordinates for those in a cluster rest frame, and "untilded" coordinates for the overall center of momentum frame. These frames are all chosen to coincide at time $t=0$. For a cluster moving with velocity v in the z direction of the overall center of momentum frame, the cluster rest frame (tilded) and center of momentum frame (untilded) coordinates are related by

$$\tilde{z}=\left[\frac{E}{m}\right]z, \quad \tilde{x}=x, \quad \tilde{y}=y , \tag{3.6}$$

where m is the cluster mass, and E is the cluster energy in the overall center of momentum frame. Since the Lorentz contraction does not affect the coordinates perpendicular to the cluster momenta, in the following discussion we only consider the dependence on the z direction of a Gaussian wave function.

A wave function in the cluster rest frame is defined as

$$\tilde{\psi}(\tilde{z})=\tilde{n}\exp\left[-\frac{1}{2R^2}\tilde{z}^2\right] . \tag{3.7}$$

Usually a wave function is normalized in the rest frame of the cluster as

$$1=\int_{-\infty}^{\infty}d\tilde{z}\,\tilde{\psi}^2(\tilde{z}) \tag{3.8}$$

so that

$$\tilde{n}=\left[\frac{1}{\pi R^2}\right]^{1/4} . \tag{3.9}$$

We consider such a cluster wave function in the center of momentum coordinate z by rewriting Eq. (3.6) as

$$\tilde{z}^2=\frac{z^2}{1-v^2} , \tag{3.10}$$

where the velocity of light is taken as $c=1$. Now we require that the cluster wave function is normalized to unity in the overall center of momentum frame. Then instead of the normalization of Eq. (3.8), we have

$$1=\int_{-\infty}^{\infty}dz\,\psi^2(z) , \tag{3.11}$$

where

$$\psi(z)=n\exp\left[-\frac{1}{2R^2(1-v^2)}z^2\right] . \tag{3.12}$$

For this normalization to hold, $n=(E/m)^{1/2}\tilde{n}$. We now Fourier transform the cluster wave function into momentum space using

$$\begin{aligned}\phi(q_z)&=\int_{-\infty}^{\infty}dz\exp(iq_z z)\psi(z)\\&=n\exp\left[-\frac{R^2(1-v^2)}{2}q_z^2\right][2\pi R^2(1-v^2)]^{1/2}\end{aligned} \tag{3.13}$$

or

$$\begin{aligned}\phi(q_z)=&(\pi R^2)^{1/4}\sqrt{2}\exp\left[-\frac{R^2}{2}q_z^2\right]\\&\times\exp\left[\frac{v^2R^2}{2}q_z^2\right]\left[\frac{m}{E}\right]^{1/2} .\end{aligned} \tag{3.14}$$

When extending the above derivation to the three-dimensional momentum space, a quark-antiquark cluster wave function, that is, a Gaussian in the cluster rest frame, is described as follows. The quark and antiquark have momenta $\mathbf{q}_1'$ and $\mathbf{q}_7'$ in the overall center of momentum frame, which combine to form the meson momentum as

$$\mathbf{p}_\alpha=\mathbf{q}_1'+\mathbf{q}_7' . \tag{3.15}$$

Thus we obtain for the meson wave function [Eq. (3.3)] in momentum space, in the overall center of momentum frame,

$$\begin{aligned}\phi_\alpha(\mathbf{p}_\alpha,\mathbf{q}_1',\mathbf{q}_7')=&C_\alpha\exp[-\tfrac{1}{4}R_m^2(\mathbf{q}_1'-\mathbf{q}_7')^2]\chi^{(1)}\tilde{\chi}^{(7)\dagger}\\&\times\exp\{\tfrac{1}{4}R_m^2v_\alpha^2[(\mathbf{q}_1'-\mathbf{q}_7')\cdot\hat{\mathbf{p}}_\alpha]^2\}\\&\times\left[\frac{m_\alpha}{E_\alpha}\right]^{1/2} .\end{aligned} \tag{3.16}$$

Here $\hat{\mathbf{p}}_\alpha$ is the unit vector in the direction of $\mathbf{p}_\alpha$, and v_α is the velocity of the meson cluster, where $\chi^{(1)}$ and $\tilde{\chi}^{(7)\dagger}$ are the two-component spinors of the quark and the antiquark. C_α is the three-dimensional rest frame normalization of the wave function and the last two factors in Eq. (3.16) show the effects of the Lorentz contraction. The meson momentum $\mathbf{p}_\alpha$ is taken in an arbitrary direction, not just parallel to the z axis. The last exponential factor in Eq. (3.16) accounts for the contraction of the wave function in the direction of the cluster momentum $\mathbf{p}_\alpha$. R_m is the same constant as the one defined in Sec. II, which is related to the meson cluster size in its rest frame. The exponential factor is always greater than unity. The last factor $(m_\alpha/E_\alpha)^{1/2}$ comes from the combined effects of normalizing the moving cluster wave function to unity in the overall center of momentum frame [Eq. (3.11)], and from Fourier transforming the Lorentz contracted wave function into momentum space [Eq. (3.13)].

For a nucleon cluster wave function, describing three quarks with momenta $\mathbf{q}_1,\mathbf{q}_2$, and $\mathbf{q}_3$ in the center of momentum frame, the nucleon momentum is

$$\mathbf{P}_N=\mathbf{q}_1+\mathbf{q}_2+\mathbf{q}_3 . \tag{3.17}$$

Using Jacobi coordinates, the spatial part of the wave function in Eq. (3.2) is given by

$$\phi_N(\mathbf{P}_N,\mathbf{q}_1,\mathbf{q}_2,\mathbf{q}_3)=C_N \exp[-\tfrac{1}{4}R_N^2(\mathbf{q}_1-\mathbf{q}_2)^2-\tfrac{1}{12}R_N^2(\mathbf{q}_1+\mathbf{q}_2-2\mathbf{q}_3)^2]$$
$$\times \exp(v_N^2\{\tfrac{1}{4}R_N^2[(\mathbf{q}_1-\mathbf{q}_2)\cdot\hat{\mathbf{P}}_N]^2+\tfrac{1}{12}R_N^2[(\mathbf{q}_1+\mathbf{q}_2-2\mathbf{q}_3)\cdot\hat{\mathbf{P}}_N]^2\}) \left[\frac{m_N}{E_N}\right]\chi^{(1)}\chi^{(2)}\chi^{(3)} . \tag{3.18}$$

Here $E_N^2=P_N^2+m_N^2$, where E_N is the nucleon energy in the overall center of momentum frame and m_N is the nucleon mass. R_N is a Gaussian size parameter fitted to the rms radius of the nucleon in its own rest frame (see Sec. II). Each of the Jacobi coordinates has undergone a Lorentz contraction in the direction of the nucleon momentum $\mathbf{P}_N$, and hence the last factor is (m_N/E_N) rather than the square root of it as in the two-body meson cluster case. v_N is the velocity of the nucleon cluster in the overall center of momentum frame. C_N is the normalization as determined in the nucleon rest frame. Thus we can express both the two-body meson cluster wave function, Eq. (3.16), and the three-body nucleon cluster wave function, Eq. (3.18), as a rest frame wave function times factors accounting for the Lorentz contraction along the direction of the cluster momenta.

In this work we take into account the Lorentz contraction of the meson cluster wave functions only since the effects from the contraction of the nucleon cluster wave functions are negligible due to the small nucleon (antinucleon) velocity at the energy considered here. By inserting the Lorentz contracted meson wave function of Eq. (3.16) into the defining Eq. (3.1) of the annihilation amplitude, we finally obtain the transition matrix element for $P\bar{P}$ annihilation into two mesons as

$$T=N^{(0)}_{N\bar{N}\alpha\beta}\delta^3(\mathbf{P}_N+\mathbf{P}_{\bar{N}}-\mathbf{p}_\alpha-\mathbf{p}_\beta)\exp\left[-\frac{3R_N^2R_m^2}{2(3R_N^2+4R_m^2)}(\tfrac{2}{3}\mathbf{P}_N)_\perp^2-\frac{3R_N^2\tilde{R}_m^2}{2(3R_N^2+4\tilde{R}_m^2)}(\mathbf{p}_\alpha-\tfrac{2}{3}\mathbf{P}_N)_\parallel^2\right]$$
$$\times\left[\frac{\pi^2}{AB}\right]^{3/2}\frac{(3R_N^2+2R_m^2)(R_N^2+2R_m^2)}{B(3R_N^2+4R_m^2)(R_N^2+R_m^2)}\tilde{\lambda}_{A2}\left[\frac{A}{\tilde{A}}\right]^{1/2}\left[\frac{B}{\tilde{B}}\right]^{1/2}\left[\frac{m_\alpha m_\beta}{E_\alpha E_\beta}\right]^{1/2}M(v_\alpha,v_\beta) , \tag{3.19}$$

where

$$\tilde{R}_m^2=\left[1-\frac{v_\alpha^2+v_\beta^2}{2}\right]R_m^2,\quad \tilde{A}=\tfrac{1}{2}(R_N^2+\tilde{R}_m^2),\quad \tilde{B}=\frac{2R_N^2(3R_N^2+4\tilde{R}_m^2)}{(R_N^2+\tilde{R}_m^2)} . \tag{3.20}$$

Here v_α and v_β are the velocities of the meson clusters α and β, and $(\mathbf{P}_N)_\perp$ and $(\mathbf{P}_N)_\parallel$ are the transverse and the longitudinal components of $\mathbf{P}_N$ with respect to the direction of the meson momentum $\mathbf{p}_\alpha$

$$(\mathbf{P}_N)_\parallel=(\mathbf{P}_N\cdot\hat{\mathbf{p}}_\alpha)\hat{\mathbf{p}}_\alpha,\quad (\mathbf{P}_N)_\perp=\mathbf{P}_N-(\mathbf{P}_N\cdot\hat{\mathbf{p}}_\alpha)\hat{\mathbf{p}}_\alpha . \tag{3.21}$$

The normalization factor $N^{(0)}_{N\bar{N}\alpha\beta}$ is defined by taking the limit $\beta_N=\beta_m=0$ of $N_{N\bar{N}\alpha\beta}$ as given in the Appendix [see Eq. (A22)]. The spin-flavor matrix element is derived as

$$M(v_\alpha,v_\beta)=\boldsymbol{\sigma}^{(2)}\cdot\boldsymbol{\sigma}^{(3)}\boldsymbol{\sigma}^{(7)}\cdot\mathbf{p}_\alpha(1+Z^m_{(1)})+Q^m_{(23)(7)}V^m_{(1)}$$
$$+D^m_{(2)}\{(\boldsymbol{\sigma}^{(2)}\cdot\boldsymbol{\sigma}^{(7)}\boldsymbol{\sigma}^{(3)}\cdot\mathbf{p}_\alpha+\boldsymbol{\sigma}^{(3)}\cdot\boldsymbol{\sigma}^{(7)}\boldsymbol{\sigma}^{(2)}\cdot\mathbf{p}_\alpha)(1+Z^m_{(2)})+(Q^m_{(27)(3)}+Q^m_{(37)(2)})V^m_{(2)}\}$$
$$+D^N_{(1)}\{\boldsymbol{\sigma}^{(2)}\cdot\boldsymbol{\sigma}^{(3)}\boldsymbol{\sigma}^{(7)}\cdot\mathbf{P}_N(1+Z^N_{(1)})+Q^N_{(23)(7)}V^N_{(1)}$$
$$+(\boldsymbol{\sigma}^{(2)}\cdot\boldsymbol{\sigma}^{(7)}\boldsymbol{\sigma}^{(3)}\cdot\mathbf{P}_N+\boldsymbol{\sigma}^{(3)}\cdot\boldsymbol{\sigma}^{(7)}\boldsymbol{\sigma}^{(2)}\cdot\mathbf{P}_N)(1+Z^N_{(2)})+(Q^N_{(27)(3)}+Q^N_{(37)(2)})V^N_{(2)}\} , \tag{3.22}$$

where

$$Z^m_{(1)}=\frac{4R_N^2(-\tilde{R}_m^2+R_m^2)(9R_N^4+15R_N^2\tilde{R}_m^2+21R_N^2R_m^2+32R_m^2\tilde{R}_m^2)}{3(3R_N^2+4\tilde{R}_m^2)^2(3R_N^2+2R_m^2)(R_N^2+2R_m^2)} ,$$
$$Z^m_{(2)}=-\frac{(-\tilde{R}_m^2+R_m^2)(27R_N^4+24R_N^2\tilde{R}_m^2-16R_m^2\tilde{R}_m^2)}{3R_m^2(3R_N^2+4\tilde{R}_m^2)^2} ,$$
$$V^m_{(1)}=\frac{4R_N^2(-\tilde{R}_m^2+R_m^2)(3R_N^2+4R_m^2)(3R_N^2+2\tilde{R}_m^2)}{\sqrt{15}(3R_N^2+4\tilde{R}_m^2)^2(3R_N^2+2R_m^2)(R_N^2+2R_m^2)} ,$$
$$V^m_{(2)}=-\frac{8\tilde{R}_m^2(-\tilde{R}_m^2+R_m^2)(3R_N^2+4R_m^2)}{\sqrt{15}R_m^2(3R_N^2+4\tilde{R}_m^2)^2} ,$$
$$D^m_{(2)}=\frac{R_N^2R_m^2}{(3R_N^2+2R_m^2)(R_N^2+2R_m^2)} ,$$

$$Z^N_{(1)}=Z^N_{(2)}=\frac{2(-\tilde{R}^{\,2}_m+R^2_m)(9R^4_N+16R^2_N\tilde{R}^{\,2}_m+32R^2_NR^2_m+48R^2_m\tilde{R}^{\,2}_m)}{9(3R^2_N+4\tilde{R}^{\,2}_m)^2(R^2_N+2R^2_m)}\ ,$$

$$V^N_{(1)}=V^N_{(2)}=-\frac{16R^2_N(-\tilde{R}^{\,2}_m+R^2_m)^2}{15(3R^2_N+4\tilde{R}^{\,2}_m)^2(R^2_N+2R^2_m)}\ ,\tag{3.23}$$

$$D^N_{(1)}=-\frac{R^2_N}{(3R^2_N+2R^2_m)}\ ,$$

$$Q^m_{(ij)(k)}=\sum_{\mu_i\mu_j\mu_k}(-1)^{\mu_i+\mu_j+\mu_k}\sigma^{(i)}_{-\mu_i}\sigma^{(j)}_{-\mu_j}\sigma^{(k)}_{-\mu_k}(\mathbf{p}_\alpha)_{\mu_i+\mu_j+\mu_k}(1\mu_i1\mu_j|2\mu_i+\mu_j)(2\mu_i+\mu_j1\mu_k|1\mu_i+\mu_j+\mu_k)\ ,$$

$$Q^N_{(ij)(k)}=\sum_{\mu_i\mu_j\mu_k\mu}(-1)^{\mu_i+\mu_j}\sigma^{(i)}_{-\mu_i}\sigma^{(j)}_{-\mu_j}\sigma^{(k)}_{-\mu_k}(\mathbf{P}_N)_{-\mu}(1\mu_i1\mu_j|2\mu_i+\mu_j)(1\mu_k1\mu|2\mu_k+\mu)\delta_{\mu_i+\mu_j,-\mu_k-\mu}\ .$$

The terms depending on $Z^m_{(i)}$, $V^m_{(i)}$, $Z^N_{(i)}$, and $V^N_{(i)}$ describe the effects of the Lorentz contraction on the meson cluster wave functions in the spin-flavor part of the transition amplitude. In the nonrelativistic limit, i.e., in the limit $v_\alpha=v_\beta=0$ where $\tilde{R}^{\,2}_m=R^2_m$, these terms vanish due to their common factor $(-\tilde{R}^{\,2}_m+R^2_m)$. Lorentz contraction effects in the transition amplitude are formally also apparent in the modified normalization by a factor of $(AB/\tilde{A}\tilde{B})^{1/2}(m_\alpha m_\beta/E_\alpha E_\beta)^{1/2}$, and the altered exponential dependence on the momenta $\mathbf{P}_N$ and $\mathbf{p}_\alpha$, when comparing to the nonrelativistic limit.

IV. NUMERICAL RESULTS

In a nonrelativistic quark model $N\bar{N}$ annihilation data can best be described by a superposition of two- and three-meson transitions.[17] Due to kinematical reasons relativistic effects are expected to be more important in the two-meson than in the three-meson final states. In the two-meson annihilation the velocity of each meson reaches its largest value since the two mesons possess the largest available energy. We have shown in Ref. 17 that the nonrelativistic model $A2$ ($P\bar{P}\rightarrow$ two mesons, Fig. 1) with a planar topology can explain the general features of the experimental two-meson branching ratios reasonably well. Presently we examine the relativistic corrections due to the small components and the Lorentz contraction of the quark cluster wave functions to the nonrelativistic model $A2$ for $P\bar{P}$ annihilation into two mesons. The validity of a nonrelativistic quark model in a kinematical region where relativity is seemingly rather important is investigated. The subsequent uncertainties resulting from the nonrelativistic kinematics are stated quantitatively.

The effects on the transition amplitude in the $A2$ diagram, when including a small Dirac component in the cluster wave functions, are derived in Eqs. (2.13)–(2.16). The probability of the small component in the nucleon/antinucleon and meson clusters is determined by the parameters β_N and β_m. When taking the limit $\beta_N\beta_m\rightarrow 0$ and keeping the normalization $(N_{N\bar{N}\alpha\beta}\lambda_{A2}\beta^2_N\beta_m)$ fixed by readjusting the strength parameter λ_{A2}, we obtain the nonrelativistic limit of the $A2$ transition amplitude as originally defined in Ref. 17. Since the overall normalization can be adjusted by the parameter λ_{A2}, the relevant effects when introducing small components are contained in the spin-flavor matrix element $M_{\alpha\beta}(\beta_N\beta_m)$ of Eq. (2.15). When the same parameter β_m is used for all mesons, such factors as the normalization and the explicit momentum dependence in Eq. (2.13) do not account for any change in the nonrelativistic result. In order to separate off the common momentum dependence of the annihilation channels, we define a reduced spin-flavor matrix element $\tilde{M}(\beta_N\beta_m)$ by

$$M(\beta_N\beta_m)=|\mathbf{P}_N|^{L_i}|\mathbf{p}_\alpha|^{l_f}\tilde{M}(\beta_N\beta_m)\ ,\tag{4.1}$$

where L_i and l_f are the relative angular momenta of the initial proton-antiproton and the final two-meson states, respectively. Here we restrict ourselves to the two cases, $L_i=0$, $l_f=1$ and $L_i=1$, $l_f=0$, which are the dominant on-shell contributions.

In Table I the spin-flavor matrix elements $|\tilde{M}(\beta_N\beta_m)|^2$, which solely depend on the product $\beta_N\beta_m$, are shown for the two cases, $\beta_N\beta_m=0$ and $\beta_N\beta_m=(0.36)^2$. The nonrelativistic limit of the matrix elements is given by setting $\beta_N\beta_m=0$ and corresponds to that of Ref. 17. Numerical values for the spin-flavor matrix elements of Ref. 17 are slightly different from the values of Table I in the case of initial S wave, since in the previous paper we have made the approximation that the small term in Eq. (2.15) proportional to $C^m_{(2)}$ is ignored. This term yields a minor contribution by less than 10% of the total value. By defining the ratio of relativistic to nonrelativistic spin-flavor matrix element

$$t(\beta_N\beta_m)=\frac{|M(\beta_N\beta_m)|^2}{|M(\beta_N\beta_m=0)|^2}=\frac{|\tilde{M}(\beta_N\beta_m)|^2}{|\tilde{M}(\beta_N\beta_m=0)|^2}\ ,\tag{4.2}$$

the effect of the small components is estimated. The ratio $t(\beta_N\beta_m)$ is approximately the same for all meson channels with the same relative orbital angular momentum of the initial proton-antiproton state

$$t(\beta_N\beta_m=0.36^2)\sim 0.86 \text{ for } L_i=0$$
$$\sim 0.70 \text{ for } L_i=1\ , \quad (4.3)$$

as seen in Table I. The result is insensitive to sizable changes in the radii parameters R_N and R_m.

The dependence of the ratio $t(\beta_N\beta_m)$ on the small component parameters $(\beta_N\beta_m)$ is displayed in Fig. 4. As already discussed in Sec. II, positive values for $(\beta_N\beta_m)$ in

TABLE I. The effect of the small component on the spin-flavor matrix element $\tilde{M}_{\alpha\beta}(\beta_N\beta_m)$ of Eq. (4.1). The matrix elements in the nonrelativistic limit $(\beta_N\beta_m=0)$ and in the case of $\beta_N\beta_m=(0.36)^2$ are shown in the second and third column, respectively. The ratio of relativistic to nonrelativistic matrix element $t(\beta_N\beta_m)=|\tilde{M}_{\alpha\beta}(\beta_N\beta_m)|^2/|\tilde{M}_{\alpha\beta}(\beta_N\beta_m=0)|^2$ [Eq. (4.2)] is given in the fourth column. The dependence of $t[\beta_N\beta_m=(0.36)^2]$ on R_N and R_m is also shown.

	$\lvert\tilde{M}_{\alpha\beta}(\beta_N\beta_m=0)\rvert^2$	$\lvert\tilde{M}_{\alpha\beta}[\beta_N\beta_m=(0.36)^2]\rvert^2$	$t[\beta_N\beta_m=(0.36)^2]$			
R_N	0.62 fm	0.62 fm	0.62 fm	0.50 fm	0.62 fm	0.62 fm
R_m	0.57 fm	0.57 fm	0.57 fm	0.57 fm	0.50 fm	0.40 fm
$^{11}S_0$						
$\rho\rho$	1591.1	1359.1	0.85	0.87	0.85	0.85
$\omega\omega$	530.4	453.0	0.85	0.87	0.85	0.85
$^{13}S_1$						
$\rho\pi$	2700	2343.9	0.87	0.88	0.86	0.86
$\omega\eta$	900	781.3	0.87	0.88	0.86	0.86
$^{31}S_1$						
$\rho\pi$	2946.5	2516.8	0.85	0.87	0.85	0.85
$\omega\rho^0$	2946.5	2516.8	0.85	0.87	0.85	0.85
$^{33}S_1$						
$\pi^+\pi^-$	345.0	298.3	0.86	0.88	0.86	0.86
$\rho^+\rho^-$	2557.9	2188.6	0.86	0.87	0.85	0.85
$\omega\pi^0$	762.2	647.2	0.85	0.86	0.85	0.85
$\rho^0\eta$	762.2	647.2	0.85	0.86	0.85	0.85
$^{11}P_1$						
$\rho\pi$	60.56	41.81	0.69	0.69	0.69	0.71
$\omega\eta$	20.19	13.94	0.69	0.69	0.69	0.71
$^{31}P_1$						
$\rho^+\rho^-$	112.16	77.43	0.69	0.70	0.69	0.71
$\rho^0\eta$	56.08	38.71	0.69	0.70	0.69	0.71
$\omega\pi^0$	56.08	38.71	0.69	0.70	0.69	0.71
$^{13}P_0$						
$\pi\pi$	817.62	569.26	0.70	0.70	0.70	0.72
$\rho\rho$	272.54	189.75	0.70	0.70	0.70	0.72
$\eta\eta$	272.54	189.75	0.70	0.70	0.70	0.72
$\omega\omega$	90.85	63.25	0.70	0.70	0.70	0.72
$^{13}P_1$						
$^{13}P_2$						
$\rho\rho$	392.45	271.32	0.69	0.70	0.70	0.71
$\omega\omega$	130.82	90.44	0.69	0.70	0.70	0.71
$^{33}P_0$						
$\eta\pi^0$	60.56	41.46	0.68	0.69	0.69	0.71
$\omega\rho^0$	20.19	13.82	0.68	0.69	0.69	0.71
$^{33}P_1$						
$\rho\pi$	224.31	155.25	0.69	0.70	0.70	0.71
$^{33}P_2$						
$\omega\rho^0$	158.27	109.20	0.69	0.69	0.69	0.71

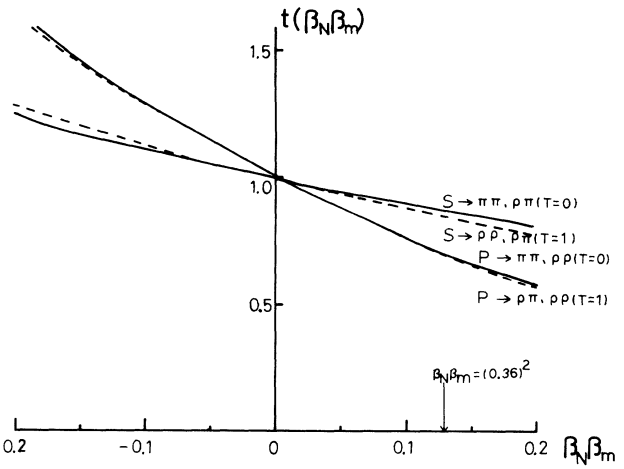

FIG. 4. The effects of the small components on the ratio of the spin-flavor part in Eq. (4.2): $t(\beta_N\beta_m) = |\tilde{M}_{\alpha\beta}(\beta_N\beta_m)|^2/|\tilde{M}_{\alpha\beta}(\beta_N\beta_m=0)|^2$. The typical channels, $L_i \to \pi\pi$, $\rho\pi$, and $\rho\rho$, are shown, where L_i is the relative angular momentum of the initial nucleon-antinucleon state. Negative values of $(\beta_N\beta_m)$ correspond to the case of Eq. (2.18). Here $R_N = 0.62$ fm and $R_m = 0.57$ fm.

Eq. (2.15) correspond to interacting, continuous quark (antiquark) lines in the $A2$ transition (labeled by 1 and 4 in Fig. 1). In the case of negative values for $(\beta_N\beta_m)$ the connecting quark (antiquark) lines describe true, noninteracting spectator particles (the single quark wave function overlap is normalized to unity.) The indication of the positive value $(0.36)^2$ in Fig. 4 is just meant to point out quantitatively the physically relevant case, i.e., where this particular value of $\beta_N\beta_m$ reproduces the probability of the lower component in the bag model. Equally well a negative value has to be chosen when considering noninteracting spectator particles.

The two-meson transitions from initial S and P wave are affected differently when considering the $(\beta_N\beta_m)$ dependence. In the region where $\beta_N\beta_m > 0$ S-wave annihilation into two mesons is enhanced with respect to P-wave annihilation. For $\beta_N\beta_m < 0$ the two-meson transitions from P-wave annihilation become stronger than from S wave when comparing to the nonrelativistic limit $(\beta_N\beta_m = 0)$. The relative weight of the two partial wave amplitudes depends on the sign of $(\beta_N\beta_m)$, i.e., on the treatment of the continuous quark (antiquark) lines (interacting or noninteracting). The initial state P-wave annihilation decreases with increasing $(\beta_N\beta_m)$ more rapidly than the S-wave annihilation. For a physically reasonable value of $\beta_N\beta_m = (0.36)^2$ (which corresponds to a center of momentum uncorrected axial charge $g_A/g_V = 1.30$), assuming a scalar interaction for all quark (antiquark) lines, the enhancement of S-wave relative to P-wave annihilation is by a factor of $0.86/0.7 = 1.2$.

The change of the absolute value of the spin-flavor matrix element for a selected partial wave when including the relativistic small component can be recovered by readjusting the strength of the $A2$ annihilation interaction λ_{A2} in Eq. (2.13). Therefore, effects of the small component on the quark wave functions do not change the results of the meson branching ratios in initial states with the same relative orbital angular momentum. However, the relative weight of the annihilation amplitudes of the initial S and P waves is modified to the order of 20%. When considering, especially quantitatively, the physical meaning of the strength parameter λ_{A2}, relativistic corrections become very relevant and necessarily have to be included in the model. In order to obtain further predictions for the partial annihilation cross sections of the final meson states one has to take into account the initial state interaction and the corresponding background from the three-meson annihilation of the proton-antiproton system.

In the work of Green *et al.*[22] the so-called rearrangement topology for the transition of the $N\bar{N}$ system into two mesons is considered, where one $q\bar{q}$ pair in the initial state is annihilated and none in the final state are created. In the present work we consider the annihilation model $A2$, which in the nonrelativistic approach can explain the experimental annihilation data best.[17] In the relativistic extension of their model, by including a small component, Green *et al.* employ two- and three-quark cluster wave functions which are not explicitly center of momentum eigenstates of the total cluster momentum. In the present approach a projection technique is applied to construct cluster momentum eigenstates in order to guarantee translational invariance. These center of momentum corrections are generally known to be large, therefore a proper treatment of this problem is essential when including relativity. Despite these obvious differences in the model approaches employed in the present paper and by the authors of Ref. 22, in a wider sense parallel results are obtained. Green *et al.*, conclude that the relativistic extension of the $^3P_0$ vertex yields minor contributions when comparing to the nonrelativistic limit in the specific partial wave of the initial state. Accordingly, we conclude that the introduction of small components in the quark wave functions has little influence on predictions of relative ratios of annihilation amplitudes in the same relative angular momentum state of the initial $p\bar{p}$ system.

The effects of the Lorentz contraction on the cluster wave functions as derived for the transition amplitude are calculated by using Eqs. (3.19)–(3.23). At the low values for the center of mass energy considered ($T_{\text{c.m.}} < 150$ MeV), the two mesons in the final state are moving quite relativistically while the nucleon/antinucleon can still be treated nonrelativistically. The respective nucleon velocities ($c = 1$)

$$v_N = 0.23 \text{ at } T_{\text{c.m.}} = 50 \text{ MeV}$$
$$= 0.38 \text{ at } T_{\text{c.m.}} = 150 \text{ MeV}, \tag{4.4}$$

are considerably smaller than the corresponding meson velocities v_α and v_β given in Table II. Therefore, the effects of the Lorentz contraction are taken into account for the meson cluster wave functions only. In Table II we present results for the ratio of relativistic to nonrelativistic transition amplitude

TABLE II. The effects of the Lorentz contraction in the transition $L_i \to ss$ at $T_{\text{c.m.}}=50$ MeV ($P_N=218$ MeV/c), where s is one of the s-wave mesons. The ratio $w(v_\alpha,v_\beta)=|T_{\text{rel}}|^2/|T_{\text{non}}|^2$ [Eq. (4.5)] is shown where T_{non} is the nonrelativistic limit (without Lorentz contraction) which is obtained by setting $v_\alpha=v_\beta=0$ in $T_{\text{rel}}(c=1)$. The partial contributions from the spin-flavor part and the spatial part to $w(v_\alpha,v_\beta)$ are also shown. The product of the two numbers results in $w(v_\alpha,v_\beta)$. The symbols ($S=0$) and ($S=1$) specify the spin singlet and triplet production. In the initial P state the values in both spin states are the same.

Mesons α,β	$\pi\pi$	$\rho\pi$	$\rho\rho$
p_α	953 MeV	802 MeV	579 MeV
velocity v_α,v_β	0.989,0.989	0.722,0.985	0.601,0.601
$(m_\alpha m_\beta/E_\alpha E_\beta)^{1/2}$	0.145	0.344	0.799
	($R_N=0.62$ fm, $R_m=0.57$ fm)		
$S\to ss$			
$w(v_\alpha,v_\beta)$	2.00	$1.15_{(S=1)}$, $1.06_{(S=0)}$	$1.16_{(S=1)}$, $1.15_{(S=0)}$
spatial part	1.23	0.82	1.03
spin-flavor part	1.63	$1.41_{(S=1)}$, $1.30_{(S=0)}$	$1.12_{(S=1)}$, $1.12_{(S=0)}$
$P\to ss$			
$w(v_\alpha,v_\beta)$	2.04	1.13	1.17
spatial part	1.23	0.82	1.03
spin-flavor part	1.66	1.38	1.13
	($R_N=0.50$ fm, $R_m=0.57$ fm)		
$S\to ss$			
$w(v_\alpha,v_\beta)$	1.36	$0.91_{(S=1)}$, $0.85_{(S=0)}$	$1.12_{(S=1)}$, $1.12_{(S=0)}$
spatial part	0.74	0.61	0.98
spin-flavor part	1.83	$1.49_{(S=1)}$, $1.39_{(S=0)}$	$1.14_{(S=1)}$, $1.13_{(S=0)}$
$P\to ss$			
$w(v_\alpha,v_\beta)$	1.58	0.96	1.16
spatial part	0.74	0.61	0.98
spin-flavor part	2.13	1.57	1.18
	($R_N=0.62$ fm, $R_m=0.50$ fm)		
$S\to ss$			
$w(v_\alpha,v_\beta)$	1.10	$0.92_{(S=1)}$, $0.85_{(S=0)}$	$1.10_{(S=1)}$, $1.10_{(S=0)}$
spatial part	0.73	0.68	1.00
spin-flavor part	1.51	$1.36_{(S=1)}$, $1.25_{(S=0)}$	$1.11_{(S=1)}$, $1.10_{(S=0)}$
$P\to ss$			
$w(v_\alpha,v_\beta)$	1.07	0.88	1.10
spatial part	0.73	0.68	1.00
spin-flavor part	1.47	1.29	1.11
	($R_N=0.62$ fm, $R_m=0.40$ fm)		
$S\to ss$			
$w(v_\alpha,v_\beta)$	0.43	$0.61_{(S=1)}$, $0.57_{(S=0)}$	$1.00_{(S=1)}$, $0.99_{(S=0)}$
spatial part	0.32	0.48	0.93
spin-flavor part	1.35	$1.26_{(S=1)}$, $1.17_{(S=0)}$	$1.08_{(S=1)}$, $1.07_{(S=0)}$
$P\to ss$			
$w(v_\alpha,v_\beta)$	0.41	0.57	0.99
spatial part	0.32	0.48	0.93
spin-flavor part	1.27	1.18	1.07

$$w(v_\alpha,v_\beta)=\frac{|T_{\text{rel}}|^2}{|T_{\text{non}}|^2} \tag{4.5}$$

at an energy of $T_{\text{c.m.}}=50$ MeV. T_{rel} is defined as the partial wave amplitude of T in Eq. (3.19) and T_{non} as the appropriate nonrelativistic limit of T_{rel} for vanishing meson velocities, i.e., $v_\alpha=v_\beta=0$ in T_{rel}. The respective contributions to $w(v_\alpha,v_\beta)$ are from the ratio of the spin-flavor parts $|M(v_\alpha,v_\beta)/M(0,0)|^2$ of Eq. (3.22) and the ratio of the spatial parts

$$\left|\frac{T(v_\alpha,v_\beta)}{M(v_\alpha,v_\beta)}\Big/\frac{T(0,0)}{M(0,0)}\right|^2$$

of Eq. (3.19). The product of these two ratios yields the value for $w(v_\alpha, v_\beta)$. The dependence of $w(v_\alpha, v_\beta)$ on the geometrical parameters R_N and R_m is due to a complex interplay of the spin-flavor coefficients and the energy-dependent normalization factors. Results for $w(v_\alpha, v_\beta)$ are shown for selected two-meson channels ($\pi\pi$, $\rho\pi$, and $\rho\rho$) in annihilation from relative S and P waves as calculated for several nucleon/antinucleon and meson radii determined by R_N and R_m.

Lorentz contraction effects are most important in the two-pion final state, since the meson velocity almost reaches to the speed of light ($v_\pi \sim 0.99$). As a result, due mainly to the increase of the spin-flavor part, the two-pion production is enhanced by a factor of 2 as compared to other channels containing vector mesons at cluster size parameters of $R_N = 0.62$ fm and $R_m = 0.57$ fm, as used in Ref. 17. A decrease in either the nucleon or the meson radius from these original values leads to a reduction of the ratio $w(v_\alpha, v_\beta)$ for a given meson channel. The more massive the meson channels are, the weaker this effect is. Since only the meson wave functions are Lorentz contracted, a reduction in R_m has a quantitatively stronger effect on $w(v_\alpha, v_\beta)$ than an equivalent decrease in R_N. A change in the geometrical factors R_N and R_m also influences the relative weight of the considered meson channels. Large numbers for either one of the cluster radii, as in the range of values used, lead to an enhancement of the two-pion annihilation amplitude. A choice of small R_N or R_m has the opposite effect. For the intermediate values of $R_N = 0.62$ fm and $R_m = 0.50$ fm, Lorentz contraction is negligible on a 10%, level. The partial wave dependence of the relativistic transition amplitude in comparison to its nonrelativistic limit remains unaltered within $\sim 10\%$, i.e., $w(S \to ss) \approx w(P \to ss)$ for the cluster radii and annihilation channels considered.

The energy dependence of the ratio $w(v_\alpha, v_\beta)$ for the original choice of R_N and R_m in Ref. 17 is depicted in Fig. 5. Clearly, for increasing energy Lorentz contraction effects will be more important, i.e., the enhancement of the two-pion channel becomes stronger. Again, the partial wave dependence of the annihilation amplitudes as described in the nonrelativistic limit remains nearly unchanged when including the energy-dependent Lorentz contraction mechanism.

The lightest meson, the pion, due to its Goldstone boson character, is known to have an internal quark structure which is considerably different from that of other mesons.[37] The rms radius of the $q\bar{q}$ component of the pion wave function is quoted to be smaller than that of the other s and p-wave mesons [$\langle r^2 \rangle_\pi^{1/2} \leq 0.4$ fm (Ref. 37)]. The smaller pion radius consequently introduces a suppression of the two-pion annihilation amplitude due to Lorentz contraction effects. However, the two-pion production makes up only a minor part ($\sim 0.3\%$) of the total annihilation of a proton-antiproton pair into mesons. Therefore, the inclusion of the Lorentz contraction in an originally nonrelativistic $A2$ model for the cluster radii of Ref. 17, with the pion radius possibly smaller, does not change the general features of the meson branching ratios.

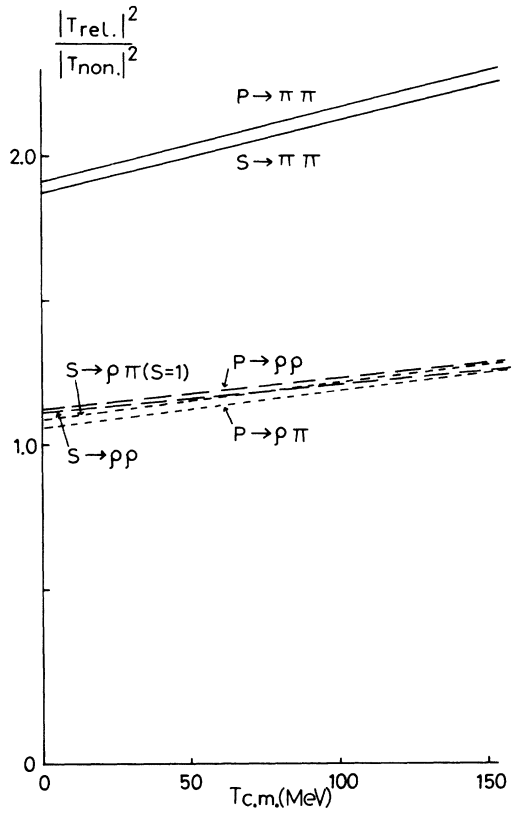

FIG. 5. Energy dependence of the Lorentz contraction effects on the ratio $w(v_\alpha, v_\beta) = |T_{\rm rel}|^2 / |T_{\rm non}|^2$ as a function of center of mass energy $T_{\rm c.m.}$. Here $R_N = 0.62$ fm and $R_m = 0.57$ fm.

The application of the Lorentz boost to the meson wave function introduces an altered dependence on the meson momentum $\mathbf{p}_\alpha$ into the transition amplitude. Consequently the angular dependence of the exponential factor in T of Eq. (3.19) will be changed when inserting the boost effect. Qualitatively Lorentz contraction enhances the backward production of mesons in the transition amplitude (as seen relative to $\mathbf{P}_N$ in the overall center of momentum frame), again with the effect being strongest in the lightest annihilation channel, the two-pion final state. Therefore, predictions for the differential cross sections of the two-meson final states will be sensitively affected. In order to obtain quantitative results for the differential cross sections in the two-meson production all partial wave amplitudes, including distortion effects due to initial and final state interaction, have to be taken in interference. A more elaborate analysis, which is beyond the scope of the present paper, is necessary to study the apparently strong influence of the Lorentz boost on the differential cross sections.

Due to the approximate treatment of the Lorentz contraction we have to remark on the normalization of the cluster wave functions. According to Eq. (3.11) we require that the wave functions of the moving clusters are normalized to unity in the overall center of momentum frame. Thus in momentum space we obtain an energy-

dependent factor of $(m/E)^{1/2}$ in the wave function of each meson cluster as shown in Eq. (3.16). Such a factor is essential and gives a large contribution to the annihilation amplitude as shown in Table II. Due to the lack of a covariant formalism of the $A2$ annihilation model, this factor will in general be frame dependent. Hence the energy dependence of the cluster wave functions is defined by the particular Lorentz frame where we choose the normalization. The relativistic Lorentz contraction effects in application to the electromagnetic form factors of the nucleon were investigated by Mitra *et al.*[27] and Stanley *et al.*[28] Following the original suggestion by Licht *et al.*,[26] the frame adopted in these calculations is the Breit frame, the center of momentum frame of the ingoing and outgoing nucleon. The proper choice of the frame together with suitable symmetry arguments of the form factor definition[27] yield the correct scaling behavior of the form factors at large q^2. In choosing the center of momentum frame in the two-meson annihilation, the calculation presented here is consistent with the previous works applying a Lorentz contraction prescription to a nonrelativistic quark model.

V. CONCLUSIONS

The conventional study of the proton-antiproton annihilation mechanism consists of a nonrelativistic quark model with a suitably defined dynamics. Particularly in the phenomenology of the two-body annihilation the nonrelativistic planar $A2$ model succeeds in describing the experimental two-meson branching ratios reasonably well. However, proton-antiproton annihilation into two mesons at rest or in flight takes place in a kinematical region where *a priori* relativistic effects are expected to play a considerable role.

By taking Dirac spinors for the single quark wave functions we define a relativistic quark annihilation model, which agrees with the planar $A2$ model in the nonrelativistic limit. The introduction of a relativistic small component in the wave function leaves results for branching ratios within the same initial partial wave (S or P) unchanged when comparing to the nonrelativistic limit. The relative weight of the transition amplitudes for initial S- and P-wave annihilation is modified to the order of 20%. The sign of the relative change in the amplitudes depends on the treatment of the continuous quark lines in the $A2$ diagram.

Following earlier studies we apply an approximate treatment of the Lorentz contraction to the $N\bar{N}$ annihilation. Depending strongly on the nucleon/antinucleon and meson sizes, Lorentz contraction affects the relative weight of the produced two-meson channels when comparing to the nonrelativistic limit. The partial wave dependence of the relative production strength of a specific annihilation channel remains essentially unchanged when introducing boost corrections. For the originally applied nucleon radius of 0.62 fm and the global meson radius of 0.50 fm in Ref. 17, which corresponds to the size parameters of $R_N=0.62$ fm and $R_m=0.57$ fm, Lorentz contraction effects tend to increase the production of the light-meson channels. Especially the two-pion production will be enhanced as compared to other channels containing vector mesons. However, it should be noted that the possible assumption of a strongly reduced pion radius will result in a suppression of the pionic channels when including the Lorentz boost in the nonrelativistic $A2$ model.

Presently we concentrate on estimating relativistic effects to the meson branching ratios, as originally calculated in the nonrelativistic $A2$ model of Ref. 17. The corrections are maximally of the order of 20%, such that the nonrelativistic approach is a rather good approximation when discussing branching ratios in the $N\bar{N}$ annihilation mechanism. In general, the relativistic extensions presented here will introduce an energy dependence into the transition amplitudes which can be studied when deriving the corresponding shortrange annihilation potential. When discussing other observables, such as the characteristic energy and angular dependence of differential cross sections in the two-meson final states, relativistic effects are possibly quite sizable.

ACKNOWLEDGMENTS

This work was supported by a grant of the Deutsche Forschungsgemeinschaft under Contract No. Fa 67/10-4 and in part by the Research Center for Nuclear Physics, Osaka University.

APPENDIX

The internal wave function $\phi_N^{(ijk)}(P_N,\mathbf{q}_1,\mathbf{q}_2,\mathbf{q}_3)$ $(i,j,k=1,2)$ of a nucleon cluster as originally defined in Eq. (2.5) is given explicitly in the following. The center of momentum eigenstate of the nucleon cluster is projected out by use of the Peierls-Yoccoz method.[32] A nucleon cluster is described by a product of three single-quark wave functions

$$\Phi_N^{(ijk)}(\mathbf{R},\mathbf{r}_1,\mathbf{r}_2,\mathbf{r}_3)=u^{(i)}(\mathbf{r}_1-\mathbf{R})u^{(j)}(\mathbf{r}_2-\mathbf{R})u^{(k)}(\mathbf{r}_3-\mathbf{R}) , \tag{A1}$$

where $\mathbf{R}$ is directed to the center of the cluster and $\mathbf{r}_i$ is the position of the ith quark. The Dirac spinor component $u^{(i)}(\mathbf{r}_i)$ is defined in Eq. (2.4). The product wave function of Eq. (A1) is not a center of momentum eigenstate of the nucleon cluster. $\Phi_N^{(ijk)}(\mathbf{R},\mathbf{r}_1,\mathbf{r}_2,\mathbf{r}_3)$ is decomposed into components of plane-wave eigenstates $\Phi_N^{(ijk)}(\mathbf{P}_N,\mathbf{r}_1,\mathbf{r}_2,\mathbf{r}_3)$ of the center of momentum with a weight factor $\varphi_N(P_N)$ as

$$\Phi_N^{(ijk)}(\mathbf{R},\mathbf{r}_1,\mathbf{r}_2,\mathbf{r}_3)=\int d^3P_N \exp(i\mathbf{R}\mathbf{P}_N)\frac{m_N}{E_N}\varphi_N(P_N)\Phi_N^{(ijk)}(\mathbf{P}_N,\mathbf{r}_1,\mathbf{r}_2,\mathbf{r}_3) , \tag{A2}$$

where $\mathbf{P}_N$, E_N, and m_N are the nucleon momentum, energy, and mass, respectively. The inverse relation is

$$\Phi_N^{(ijk)}(\mathbf{P}_N,\mathbf{r}_1,\mathbf{r}_2,\mathbf{r}_3)=\frac{1}{(2\pi)^3}\frac{1}{\varphi_N(P_N)}\frac{E_N}{m_N}\int d^3R\,\exp(-i\mathbf{R}\mathbf{P}_N)\Phi_N^{(ijk)}(\mathbf{R},\mathbf{r}_1,\mathbf{r}_2,\mathbf{r}_3)\ . \tag{A3}$$

$\varphi_N(P_N)$ is defined by the plane-wave normalization condition

$$\sum_{i,j,k}\int d^3r_1 d^3r_2 d^3r_3\Phi_N^{(ijk)\dagger}(\mathbf{P}'_N,\mathbf{r}_1,\mathbf{r}_2,\mathbf{r}_3)\Phi_N^{(ijk)}(\mathbf{P}_N,\mathbf{r}_1,\mathbf{r}_2,\mathbf{r}_3)=(2\pi)^3\delta^3(\mathbf{P}'_N-\mathbf{P}_N)\frac{E_N}{m_N}\ . \tag{A4}$$

In momentum space the projected center of momentum eigenstate is given by the Fourier transformation:

$$\Phi_N^{(ijk)}(\mathbf{P}_N,\mathbf{q}_1,\mathbf{q}_2,\mathbf{q}_3)=\frac{1}{(2\pi)^9}\int d^3r_1 d^3r_2 d^3r_3\exp(i\mathbf{q}_1\mathbf{r}_1+i\mathbf{q}_2\mathbf{r}_2+i\mathbf{q}_3\mathbf{r}_3)\Phi_N^{(ijk)}(\mathbf{P}_N,\mathbf{r}_1,\mathbf{r}_2,\mathbf{r}_3)\ . \tag{A5}$$

By use of the definition of $\phi_N^{(ijk)}(P_N,\mathbf{q}_1,\mathbf{q}_2,\mathbf{q}_3)$ in Eq. (2.5) we finally obtain

$$\phi_N^{(111)}(P_N,\mathbf{q}_1,\mathbf{q}_2,\mathbf{q}_3)=\frac{(8R_N^3\pi^{3/2})^{3/2}}{(2\pi)^6(1+\frac{3}{2}\beta_N^2)^{3/2}}\frac{1}{(2\pi)^3}\frac{E_N}{m_N}\frac{1}{\varphi_N(P_N)}\exp(-\tfrac{1}{6}R_N^2P_N^2)$$
$$\times\exp[-\tfrac{1}{4}R_N^2(\mathbf{q}_1-\mathbf{q}_2)^2-\tfrac{1}{12}R_N^2(\mathbf{q}_1+\mathbf{q}_2-2\mathbf{q}_3)^2]\chi^{(1)}\chi^{(2)}\chi^{(3)}\ , \tag{A6}$$

$$\phi_N^{(112)}(P_N,\mathbf{q}_1,\mathbf{q}_2,\mathbf{q}_3)=\frac{(8R_N^3\pi^{3/2})^{3/2}}{(2\pi)^6(1+\frac{3}{2}\beta_N^2)^{3/2}}\frac{1}{(2\pi)^3}\frac{E_N}{m_N}\frac{1}{\varphi_N(P_N)}\exp[-\tfrac{1}{6}R_N^2P_N^2]$$
$$\times\exp[-\tfrac{1}{4}R_N^2(\mathbf{q}_1-\mathbf{q}_2)^2-\tfrac{1}{12}R_N^2(\mathbf{q}_1+\mathbf{q}_2-2\mathbf{q}_3)^2](\beta_N R_N)\boldsymbol{\sigma}^{(3)}\cdot\mathbf{q}_3\chi^{(1)}\chi^{(2)}\chi^{(3)}\ , \tag{A7}$$

$$\phi_N^{(122)}(P_N,\mathbf{q}_1,\mathbf{q}_2,\mathbf{q}_3)=\frac{(8R_N^3\pi^{3/2})^{3/2}}{(2\pi)^6(1+\frac{3}{2}\beta_N^2)^{3/2}}\frac{1}{(2\pi)^3}\frac{E_N}{m_N}\frac{1}{\varphi_N(P_N)}\exp(-\tfrac{1}{6}R_N^2P_N^2)$$
$$\times\exp[-\tfrac{1}{4}R_N^2(\mathbf{q}_1-\mathbf{q}_2)^2-\tfrac{1}{12}R_N^2(\mathbf{q}_1+\mathbf{q}_2-2\mathbf{q}_3)^2](\beta_N R_N)^2\boldsymbol{\sigma}^{(2)}\cdot\mathbf{q}_2\boldsymbol{\sigma}^{(3)}\cdot\mathbf{q}_3\chi^{(1)}\chi^{(2)}\chi^{(3)}\ , \tag{A8}$$

$$\phi_N^{(222)}(P_N,\mathbf{q}_1,\mathbf{q}_2,\mathbf{q}_3)=\frac{(8R_N^3\pi^{3/2})^{3/2}}{(2\pi)^6(1+\frac{3}{2}\beta_N^2)^{3/2}}\frac{1}{(2\pi)^3}\frac{E_N}{m_N}\frac{1}{\varphi_N(P_N)}\exp(-\tfrac{1}{6}R_N^2P_N^2)$$
$$\times\exp[-\tfrac{1}{4}R_N^2(\mathbf{q}_1-\mathbf{q}_2)^2-\tfrac{1}{12}R_N^2(\mathbf{q}_1+\mathbf{q}_2-2\mathbf{q}_3)^2](\beta_N R_N)^3\boldsymbol{\sigma}^{(1)}\cdot\mathbf{q}_1\boldsymbol{\sigma}^{(2)}\cdot\mathbf{q}_2\boldsymbol{\sigma}^{(3)}\cdot\mathbf{q}_3\chi^{(1)}\chi^{(2)}\chi^{(3)}\ . \tag{A9}$$

We label the three quark momenta in the nucleon as $\mathbf{q}_1$, $\mathbf{q}_2$, and $\mathbf{q}_3$. $\chi^{(i)}$ and $\boldsymbol{\sigma}^{(i)}$ are the two-component spinor and the Pauli spin matrix of the ith quark. We define

$$\varphi_N(P_N)=\frac{1}{(2\pi)^3}\left[\frac{E_N}{m_N}\right]^{1/2}\exp(-\tfrac{1}{6}R_N^2P_N^2)\left[\frac{4R_N^2\pi}{3}\right]^{3/4}[1-6a_N+20a_N^2-\tfrac{280}{9}a_N^3+(\tfrac{4}{3}a_N-\tfrac{16}{3}a_N^2+\tfrac{400}{27}a_N^3)(R_NP_N)^2$$
$$+(\tfrac{16}{27}a_N^2-\tfrac{160}{81}a_N^3)(R_NP_N)^4+\tfrac{64}{729}a_N^3(R_NP_N)^6]^{1/2}\ , \tag{A10}$$

where

$$a_N=\frac{\beta_N^2}{4+6\beta_N^2}\ . \tag{A11}$$

The factor $\exp(-\frac{1}{6}R_N^2P_N^2)$ in the expression of φ_N cancels the identical factor in $\phi_N^{(ijk)}$ such that the center of momentum motion in momentum space is represented by the δ function in Eq. (2.5), which corresponds to a plane wave.

The corresponding internal wave functions of the antinucleon cluster in the initial state are given by

$$\phi_{\bar{N}}^{(111)\dagger}(P_{\bar{N}},\mathbf{q}_4,\mathbf{q}_5,\mathbf{q}_6)=\frac{(8R_N^3\pi^{3/2})^{3/2}}{(2\pi)^6(1+\frac{3}{2}\beta_N^2)^{3/2}}\frac{1}{(2\pi)^3}\frac{E_{\bar{N}}}{m_{\bar{N}}}\frac{1}{\varphi_N(P_{\bar{N}})}\exp(-\tfrac{1}{6}R_N^2P_{\bar{N}}^2)$$
$$\times\exp[-\tfrac{1}{4}R_N^2(\mathbf{q}_4-\mathbf{q}_5)^2-\tfrac{1}{12}R_N^2(\mathbf{q}_4+\mathbf{q}_5-2\mathbf{q}_6)^2]\tilde{\chi}^{(4)\dagger}\tilde{\chi}^{(5)\dagger}\tilde{\chi}^{(6)\dagger}(\beta_N R_N)^3\boldsymbol{\sigma}^{(4)}\cdot\mathbf{q}_4\boldsymbol{\sigma}^{(5)}\cdot\mathbf{q}_5\boldsymbol{\sigma}^{(6)}\cdot\mathbf{q}_6\ , \tag{A12}$$

$$\phi_{\bar{N}}^{(112)\dagger}(P_{\bar{N}},\mathbf{q}_4,\mathbf{q}_5,\mathbf{q}_6)=\frac{(8R_N^3\pi^{3/2})^{3/2}}{(2\pi)^6(1+\frac{3}{2}\beta_N^2)^{3/2}}\frac{1}{(2\pi)^3}\frac{E_{\bar{N}}}{m_{\bar{N}}}\frac{1}{\varphi_N(P_{\bar{N}})}\exp(-\tfrac{1}{6}R_N^2P_{\bar{N}}^2)$$
$$\times\exp[-\tfrac{1}{4}R_N^2(\mathbf{q}_4-\mathbf{q}_5)^2-\tfrac{1}{12}R_N^2(\mathbf{q}_4+\mathbf{q}_5-2\mathbf{q}_6)^2]\tilde{\chi}^{(4)\dagger}\tilde{\chi}^{(5)\dagger}\tilde{\chi}^{(6)\dagger}(\beta_N R_N)^2\boldsymbol{\sigma}^{(4)}\cdot\mathbf{q}_4\boldsymbol{\sigma}^{(5)}\cdot\mathbf{q}_5\ , \tag{A13}$$

$$\phi_{\bar{N}}^{(122)\dagger}(P_{\bar{N}},\mathbf{q}_4,\mathbf{q}_5,\mathbf{q}_6)=\frac{(8R_N^3\pi^{3/2})^{3/2}}{(2\pi)^6(1+\frac{3}{2}\beta_N^2)^{3/2}}\frac{1}{(2\pi)^3}\frac{E_{\bar{N}}}{m_{\bar{N}}}\frac{1}{\varphi_N(P_{\bar{N}})}\exp(-\tfrac{1}{6}R_N^2P_{\bar{N}}^2)$$
$$\times\exp[-\tfrac{1}{4}R_N^2(\mathbf{q}_4-\mathbf{q}_5)^2-\tfrac{1}{12}R_N^2(\mathbf{q}_4+\mathbf{q}_5-2\mathbf{q}_6)^2]\tilde{\chi}^{(4)\dagger}\tilde{\chi}^{(5)\dagger}\tilde{\chi}^{(6)\dagger}(\beta_N R_N)\boldsymbol{\sigma}^{(4)}\cdot\mathbf{q}_4\ , \tag{A14}$$

$$\phi_{\bar{N}}^{(222)\dagger}(P_{\bar{N}},\mathbf{q}_4,\mathbf{q}_5,\mathbf{q}_6)=\frac{(8R_N^3\pi^{3/2})^{3/2}}{(2\pi)^6(1+\frac{3}{2}\beta_N^2)^{3/2}}\frac{1}{(2\pi)^3}\frac{E_{\bar{N}}}{m_{\bar{N}}}\frac{1}{\varphi_N(P_{\bar{N}})}\exp(-\tfrac{1}{6}R_N^2P_{\bar{N}}^2)$$
$$\times\exp[-\tfrac{1}{4}R_N^2(\mathbf{q}_4-\mathbf{q}_5)^2-\tfrac{1}{12}R_N^2(\mathbf{q}_4+\mathbf{q}_5-2\mathbf{q}_6)^2]\tilde{\chi}^{(4)\dagger}\tilde{\chi}^{(5)\dagger}\tilde{\chi}^{(6)\dagger}\ . \tag{A15}$$

In the case of the meson the factor E_N/m_N (for the baryon) in the normalization condition of Eq. (A4) is replaced by $2E_\alpha$, where E_α is the energy of the meson. The internal wave functions of a meson cluster are written as follows:

$$\phi_\alpha^{(11)}(p_\alpha,\mathbf{q}_1,\mathbf{q}_7)=\frac{(4R_m^2\pi)^{3/2}}{(2\pi)^3(1+\frac{3}{2}\beta_m^2)}\frac{1}{(2\pi)^3}\frac{2E_\alpha}{\varphi_\alpha(p_\alpha)}\exp(-\tfrac{1}{4}R_m^2p_\alpha^2)\exp[-\tfrac{1}{4}R_m^2(\mathbf{q}_1-\mathbf{q}_7)^2](\beta_m R_m)\chi^{(1)}\tilde{\chi}^{(7)\dagger}\boldsymbol{\sigma}^{(7)}\cdot\mathbf{q}_7\ , \tag{A16}$$

$$\phi_\alpha^{(12)}(p_\alpha,\mathbf{q}_1,\mathbf{q}_7)=\frac{(4R_m^2\pi)^{3/2}}{(2\pi)^3(1+\frac{3}{2}\beta_m^2)}\frac{1}{(2\pi)^3}\frac{2E_\alpha}{\varphi_\alpha(p_\alpha)}\exp(-\tfrac{1}{4}R_m^2p_\alpha^2)\exp[-\tfrac{1}{4}R_m^2(\mathbf{q}_1-\mathbf{q}_7)^2](\beta_m R_m)^2\boldsymbol{\sigma}^{(1)}\cdot\mathbf{q}_1\chi^{(1)}\tilde{\chi}^{(7)\dagger}\boldsymbol{\sigma}^{(7)}\cdot\mathbf{q}_7\ , \tag{A17}$$

$$\phi_\alpha^{(21)}(p_\alpha,\mathbf{q}_1,\mathbf{q}_7)=\frac{(4R_m^2\pi)^{3/2}}{(2\pi)^3(1+\frac{3}{2}\beta_m^2)}\frac{1}{(2\pi)^3}\frac{2E_\alpha}{\varphi_\alpha(p_\alpha)}\exp(-\tfrac{1}{4}R_m^2p_\alpha^2)\exp[-\tfrac{1}{4}R_m^2(\mathbf{q}_1-\mathbf{q}_7)^2]\chi^{(1)}\tilde{\chi}^{(7)\dagger}\ , \tag{A18}$$

$$\phi_\alpha^{(22)}(p_\alpha,\mathbf{q}_1,\mathbf{q}_7)=\frac{(4R_m^2\pi)^{3/2}}{(2\pi)^3(1+\frac{3}{2}\beta_m^2)}\frac{1}{(2\pi)^3}\frac{2E_\alpha}{\varphi_\alpha(p_\alpha)}\exp(-\tfrac{1}{4}R_m^2p_\alpha^2)\exp[-\tfrac{1}{4}R_m^2(\mathbf{q}_1-\mathbf{q}_7)^2](\beta_m R_m)\boldsymbol{\sigma}^{(1)}\cdot\mathbf{q}_1\chi^{(1)}\tilde{\chi}^{(7)\dagger}\ . \tag{A19}$$

Here we define

$$\varphi_\alpha(p_\alpha)=\frac{1}{(2\pi)^3}\sqrt{2E_\alpha}\exp(-\tfrac{1}{4}R_m^2p_\alpha^2)(2R_m^2\pi)^{3/4}[1-6a_m+15a_m^2+2a_m(1-5a_m)(R_mp_\alpha)^2+a_m^2(R_mp_\alpha)^4]^{1/2}\ , \tag{A20}$$

where

$$a_m=\frac{\beta_m^2}{4+6\beta_m^2}\ . \tag{A21}$$

By using the above notation the normalization factor $N_{N\bar{N}\alpha\beta}$ appearing in Eq. (2.13) is written as

$$N_{N\bar{N}\alpha\beta}=\left[\frac{(8R_N^3\pi^{3/2})^{3/2}}{(2\pi)^6(1+\frac{3}{2}\beta_N^2)^{3/2}}\frac{1}{(2\pi)^3}\frac{E_N}{m_N}\frac{\exp(-\frac{1}{6}R_N^2P_N^2)}{\varphi_N(P_N)}\right]^2\left[\frac{(4R_m^2\pi)^{3/2}}{(2\pi)^3(1+\frac{3}{2}\beta_m^2)}\frac{2E_\alpha}{(2\pi)^3}\frac{\exp(-\frac{1}{4}R_m^2p_\alpha^2)}{\varphi_\alpha(p_\alpha)}\right]^2\ . \tag{A22}$$

---

*Present address: Department of Physics, Faculty of Science, University of Tohoku, Sendai 980, Japan.
†Permanent address: Physics Department, University of Georgia, Athens, GA 30602.

[1]H. R. Rubinstein and H. Stern, Phys. Lett. **21**, 447 (1966).
[2]J. Harte, R. H. Socolow, and J. Vandermeulen, Nuovo Cimento **49A**, 555 (1967).
[3]M. Maruyama and T. Ueda, Nucl. Phys. **A364**, 279 (1981).
[4]M. Maruyama and T. Ueda, Phys. Lett. **124B**, 121 (1983).
[5]M. Maruyama and T. Ueda, Prog. Theor. Phys. **73**, 1211 (1985).
[6]N. Isgur and G. Karl, Phys. Rev. D **20**, 1191 (1979).
[7]C. Carlson, Phys. Rev. D **27**, 1556 (1983).
[8]C. Carlson, G. Kogut, and V. R. Pandharipande, Phys. Rev. D **27**, 233 (1983); **28**, 2807 (1983).
[9]R. Sartor and Fl. Stancu, Phys. Rev. D **34**, 3405 (1986).
[10]A. Le Yaouanc, L. Oliver, O. Pène, and J. C. Raynal, Phys. Rev. D **8**, 2223 (1973); **9**, 1415 (1974); **11**, 1272 (1975).
[11]F. Lenz *et al.*, Ann. Phys. (N.Y.) **170**, 65 (1986).
[12]A. M. Green and J. A. Niskanen, Prog. Part. Nucl. Phys. **18**, 93 (1987).
[13]A. M. Green and J. A. Niskanen, Nucl. Phys. **A412**, 448 (1984); **A430**, 605 (1984).
[14]H. Genz, Phys. Rev. D **28**, 1094 (1983).
[15]C. D. Dover, P. Fishbane, and S. Furui, Phys. Rev. Lett. **57**, 1538 (1986).
[16]M. Maruyama and T. Ueda, Prog. Theor. Phys. **78**, 841 (1987).
[17]M. Maruyama, S. Furui, and A. Faessler, Nucl. Phys. **A472**, 643 (1987).
[18]M. Maruyama, S. Furui, A. Faessler, and R. Vinh Mau, Nucl. Phys. **A473**, 649 (1987).
[19]A. M. Green, J. A. Niskanen, and S. Wycech, Phys. Lett. **139B**, 15 (1984).
[20]M. Khono and W. Weise, Nucl. Phys. **A454**, 429 (1986).

[21]E. M. Henley, T. Oka, and J. Vergados, Phys. Lett. **166B**, 274 (1986).
[22]A. M. Green, J. A. Niskanen, and S. Wycech, Phys. Lett. B **172**, 171 (1986); A. M. Green and J. A. Niskanen, Mod. Phys. Lett. A **1**, 441 (1986).
[23]R. Kokoski and N. Isgur, Phys. Rev. D **35**, 907 (1987).
[24]E. M. Henley, T. Oka, and J. D. Vergados, Nucl. Phys. **A476**, 589 (1988).
[25]K. Fujimura, T. Kobayashi, and M. Namiki, Prog. Theor. Phys. **43**, 73 (1970); **44**, 193 (1970).
[26]A. L. Licht and A. Pagnamenta, Phys. Rev. D **2**, 1150 (1970); **2**, 1156 (1970).
[27]A. N. Mitra and I. Kumari, Phys. Rev. D **15**, 261 (1977).
[28]D. P. Stanley and D. Robson, Phys. Rev. D **26**, 223 (1982).
[29]W. Glöckle, Y. Nogami, and I. Fukui, Phys. Rev. D **35**, 584 (1987).
[30]A. Buchmann, W. Leidemann, and H. Arenhövel, Nucl. Phys. **A443**, 726 (1985).
[31]T. Gutsche, M. Maruyama, and A. Fässler, Nucl. Phys. **A503**, 737 (1989).
[32]C. Wong, Phys. Rev. D **24**, 1416 (1981).
[33]G. L. Strobel and T. Pfenninger, Phys. Lett. B **195**, 7 (1987).
[34]T. De Grand *et al.*, Phys. Rev. D **12**, 2060 (1975).
[35]R. Tegen, R. Brockmann, and W. Weise, Z. Phys. A **307**, 339 (1982); R. Tegen, M. Schedl, and W. Weise, Phys. Lett. **125B**, 9 (1983); N. Barik, B. K. Dash, and M. Das, Phys. Rev. D **31**, 1652 (1985).
[36]N. Barik and B. K. Dash, Phys. Rev. D **33**, 1925 (1986); M. G. do Amaral and N. Zagury, *ibid.* **26**, 3119 (1982).
[37]V. Bernard, R. Brockmann, M. Schaden, W. Weise, and E. Werner, Nucl. Phys. **A412**, 349 (1984); V. Bernard, R. Brockmann, and W. Weise, *ibid.* **A440**, 605 (1985).